Taylor & Francis
Taylor & Francis Group

RESEARCH ARTICLE

🔓 OPEN ACCESS   ✓ Check for updates

Design, synthesis, apoptotic, and antiproliferative effects of 5-chloro-3-(2-methoxyvinyl)-indole-2-carboxamides and pyrido[3,4-b]indol-1-ones as potent EGFR^{WT}/EGFR^{T790M} inhibitors

Lamya H. Al-Wahaibi[a], Anber F. Mohammed[b], Fatema El-Zahraa S. Abdel Rahman[c], Mostafa H. Abdelrahman[d], Xuyuan Gu[e], Laurent Trembleau[e] and Bahaa G. M. Youssif[b]

[a]Department of Chemistry, College of Sciences, Princess Nourah bint Abdulrahman University, Riyadh, Saudi Arabia; [b]Pharmaceutical Organic Chemistry Department, Faculty of Pharmacy, Assiut University, Assiut, Egypt; [c]Department of Basic Sciences, Faculty of Oral and Dental Medicine, Nahda University, Beni-Suef, Egypt; [d]Pharmaceutical Organic Chemistry Department, Faculty of Pharmacy, Al-Azhar University, Assiut, Egypt; [e]School of Natural and Computing Sciences, University of Aberdeen, Aberdeen, UK

ABSTRACT

A new series of indole-2-carboxamides **5a-g**, **6a-f** and pyrido[3,4-b]indol-1-ones **7a** and **7b** have been developed as new antiproliferative agents that target both wild and mutant type EGFR. The antiproliferative effect of the new compounds was studied. **5c**, **5d**, **5f**, **5 g**, **6e**, and **6f** have the highest antiproliferative activity with GI$_{50}$ values ranging from 29 nM to 47 nM in comparison to the reference erlotinib (GI$_{50}$ = 33 nM). Compounds **5d**, **5f**, and **5 g** inhibited EGFR^{WT} with IC$_{50}$ values ranging from 68 to 85 nM while the GI$_{50}$ of erlotinib is 80 nM. Moreover, compounds **5f** and **5 g** had the most potent inhibitory activity against EGFR^{T790M} with IC$_{50}$ values of 9.5 ± 2 and 11.9 ± 3 nM, respectively, being equivalent to the reference osimertinib (IC$_{50}$ = 8 ± 2 nM). Compounds **5f** and **5 g** demonstrated excellent caspase-3 protein overexpression levels of 560.2 ± 5.0 and 542.5 ± 5.0 pg/mL, respectively, being more active than the reference staurosporine (503.2 ± 4.0 pg/mL). they also increase the level of caspase 8, and Bax while decreasing the levels of anti-apoptotic Bcl2 protein. Computational docking studies supported the enzyme inhibition results and provided favourable dual binding modes for both compounds **5f** and **5 g** within EGFR^{WT} and EGFR^{T790M} active sites. Finally, *in silico* ADME/pharmacokinetic studies predict good safety and pharmacokinetic profile of the most active compounds.

GRAPHICAL ABSTRACT
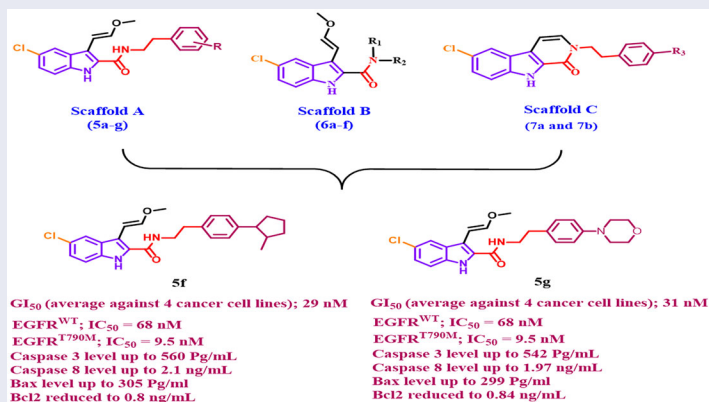
Introduction

Cancer, defined as the uncontrolled, rapid, and pathological proliferation of abnormal cells, is the second leading cause of death after cardiovascular disease[1]. Every year, cancer claims the lives of approximately 9.6 million people[2]. While significant progress has been made in the development of anticancer drugs, there are still many barriers to cancer treatment, such as poor efficacy, high toxicity, and drug resistance, all of which have had a significant impact on patients' daily lives[3]. The search for active, safe anticancer compounds with high selectivity is thus a critical issue in contemporary cancer research[4].
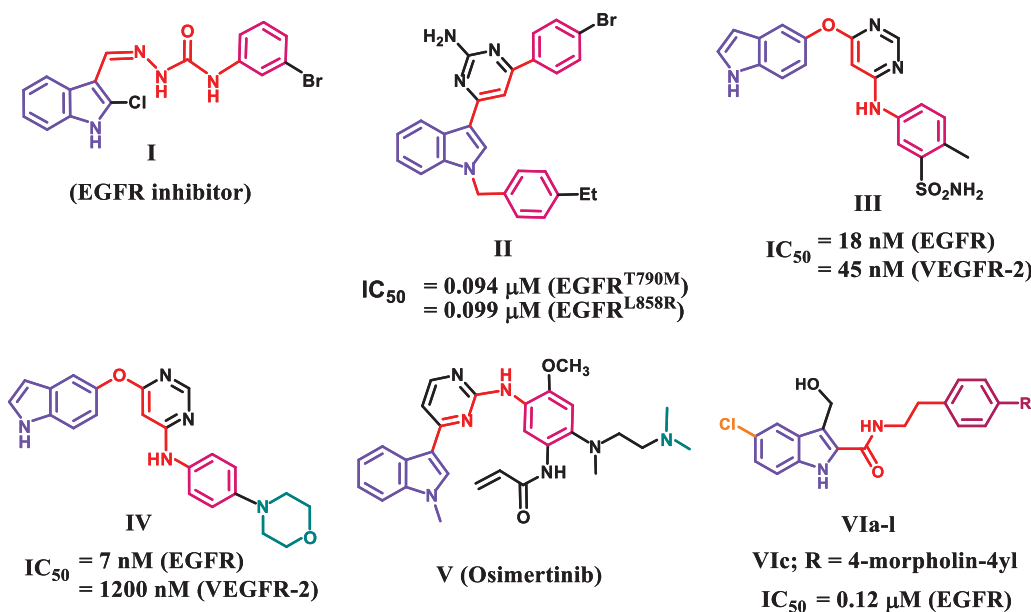
Figure 1. Structures of indole-based EGFR inhibitors **I-VI**.

As a transmembrane-bound molecule, the epidermal growth factor receptor (EGFR) regulates cell proliferation, apoptosis, migration, differentiation, and survival[5]. Increased EGFR activity caused by EGFR gene overexpression, mutation, or amplification contributes to many human cancers, including glioblastoma, epithelial cancers of the head and neck, breast cancers, and lung cancers, particularly non-small-cell lung cancers (NSCLCs)[6]. As a result, blocking the EGFR signalling pathway, either extracellularly by blocking the EGFR binding site or intracellularly by inhibiting tyrosine kinase activity, is significant in cancer prevention and treatment[7]. Advanced EGFR mutant NSCLC patients' survival has been significantly improved by first (gefitinib or erlotinib) and second (afatinib or dacomitinib)-generation EGFR tyrosine kinase inhibitors (TKIs) (Figure 1)[8,9]. But the appearance of acquired point mutations, particularly the T790 M mutation, has reduced their therapeutic efficacy and resulted in drug resistance[10]. As a result, third-generation EGFR inhibitors targeting the T790 M mutation (osimertinib and rociletinib) have been developed[11]. Unfortunately, the C797S point mutation and/or other mechanisms have been linked to acquired resistance to third-generation EGFR TKIs[12]. As a result, fourth-generation EGFR TKIs such as EAI045 and other inhibitors are being developed to provide a significant breakthrough against this mutations[13]. However, the need for novel small molecule inhibitors or therapeutic strategies to treat EGFR multipoint mutations remains unfulfilled.

On the other hand, the indole skeleton, which can be found in many active ingredients and natural products, is one of the most popular structures with potent antitumor activity[14]. Many indole derivatives are potent anticancer drugs thus far, and some of them have even been applied in clinics[15–17]. A large number of indole-based derivatives with TK inhibitory activity were also discovered in the literature review[18–21]. Li et al. reported compound **I** to have potent anticancer activity against a panel of four cancer cell lines (IC$_{50}$ = 1.43–5.48 μM)[18]. A western blot mechanistic assay of compound **I** revealed promising EGFR inhibitory activity. Compound **II** was discovered to be a dual EGFR (T790M)/c-MET inhibitor capable of targeting resistant NSCLC[19]. Compound **II** inhibited EGFR (T790M), EGFR (L858R), and c-MET with IC$_{50}$ values of 0.094, 0.099, and 0.595 μM, respectively (Figure 1).

Song et al. reported a series of indole derivatives as dual EGFR/VEGFR-2 inhibitors[20]. Compound **III** demonstrated dual inhibitory activities against EGFR and VEGFR-2, with IC$_{50}$ values of 18 and 45 nM, respectively. Compound **IV** was also reported as a dual EGFR/VEGFR-2 inhibitor, with a prominent effect against EGFR compared to **III**, indicating the significance of morpholino moiety for EGFR inhibitory activity. Osimertinib (**V**) is an EGFR TKI with a selectivity index of about 200-fold towards EGFR T790M/L858R protein over wild-type EGFR[21]. Because of its selectivity and activity, osimertinib was approved by the FDA in 2015 to treat EGFR T790M-positive NSCLC[21]. We recently[22] reported on the development of a novel series of 5-chloro-3-hydroxymethyl-indole-2-carboxamides **VIa-l** (Figure 1) as EGFR-TK antiproliferative agents. The most potent antiproliferative agent, compound **VIc** (R = 4-morpholin-4-yl), demonstrated significant EGFR inhibitory activity with an IC$_{50}$ value of 0.12 μM.

Herein, we present the synthesis and antiproliferative evaluation of a number of new 5-chloro-3–(2-methoxyvinyl)-indole-2-carboxamides **5a-g** (Scaffold A), **6a-f** (Scaffold B), and pyrido[3,4-b]indol-1-ones **7a** and **7b** (Scaffold C) derivatives as EGFR inhibitors (Figure 2). In order to increase the binding affinities of the newly designed compounds towards the EGFR active sites, the new compounds were subjected to structural modifications, including the extension of the hydroxymethyl group at C3 of compounds **VIa-l** to methoxyvinyl group. The chlorine atom in position C8 of the new compounds was retained because it produces the best results when compared to the other groups. Furthermore, amidic NH and methoxyvinyl groups were cyclized to pyridine moiety in compounds **7a** and **7b** to evaluate the effect of cyclisation on the antiproliferative action of these compounds.

MTT assay was used to assess the antiproliferative activity of the target compounds against a panel of four different cancer cell lines [A-549 (epithelial cancer cell line), MCF-7 (breast cancer cell line), Panc-1 (pancreas cancer cell line), and HT-29 (colon cancer cell line)]. Furthermore, the most active compounds were tested for EGFR (EGFR^{WT} and EGFR^{T790M}) inhibitory activity. Additionally, apoptosis assays against caspase 3, caspase 8, Bax, and antiapoptotic Bcl2 have been accomplished for the most effective compounds. Finally, docking and ADME experiments for the most active compounds will be performed to determine their binding
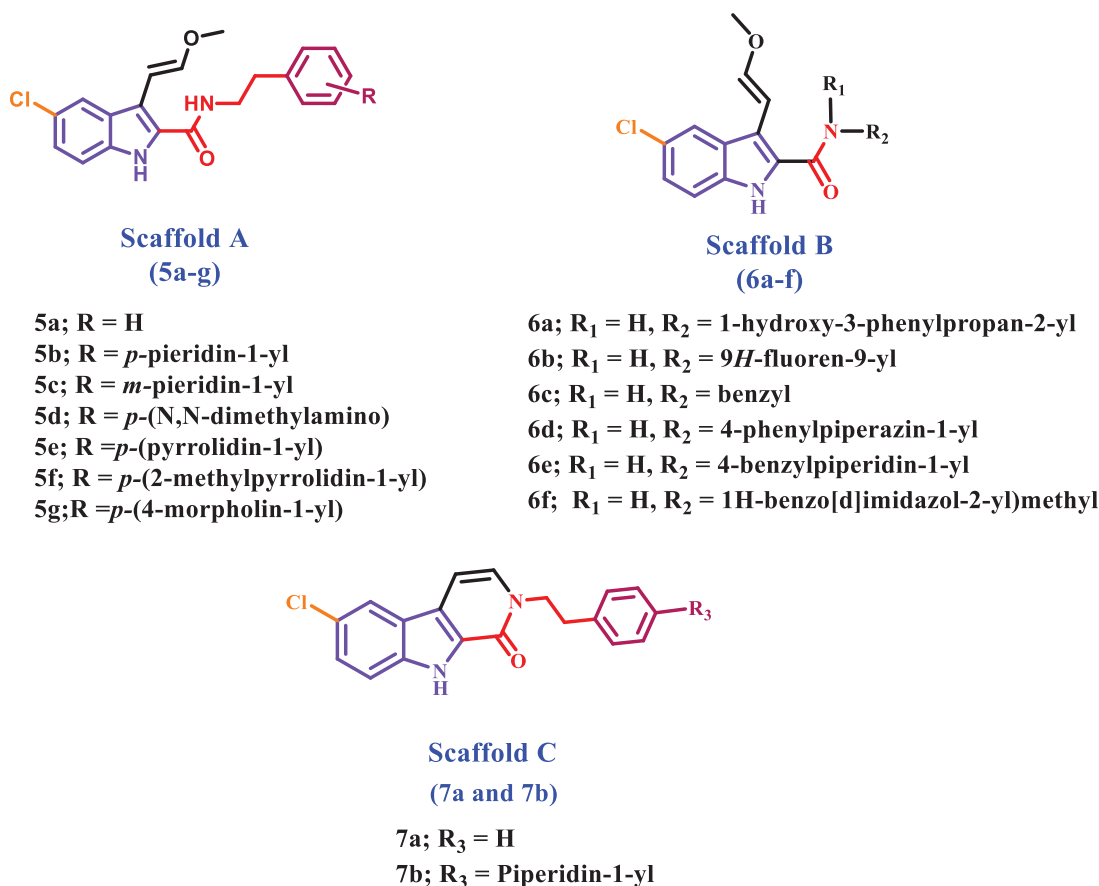
Scaffold A
(5a-g)

5a; R = H
5b; R = p-pieridin-1-yl
5c; R = m-pieridin-1-yl
5d; R = p-(N,N-dimethylamino)
5e; R =p-(pyrrolidin-1-yl)
5f; R = p-(2-methylpyrrolidin-1-yl)
5g;R =p-(4-morpholin-1-yl)

Scaffold B
(6a-f)

6a; R_1 = H, R_2 = 1-hydroxy-3-phenylpropan-2-yl
6b; R_1 = H, R_2 = 9H-fluoren-9-yl
6c; R_1 = H, R_2 = benzyl
6d; R_1 = H, R_2 = 4-phenylpiperazin-1-yl
6e; R_1 = H, R_2 = 4-benzylpiperidin-1-yl
6f; R_1 = H, R_2 = 1H-benzo[d]imidazol-2-yl)methyl

Scaffold C
(7a and 7b)

7a; R_3 = H
7b; R_3 = Piperidin-1-yl

Figure 2. Structures of new targets **5a-g**, **6a-f**, **7a**, and **7b**.

modes within the active sites of the target enzymes or to determine their pharmacokinetic and pharmacodynamic features.

Results and discussions

Chemistry

Scheme 1 describes the synthesis of target compounds **5a-g**, **6a-f**, **7a**, and **7b**. 5-chloro-3-formyl indole-2-carboxylate **(1)** was reacted with NaH and Di-*tert*-butyl dicarbonate [(Boc)$_2$O] in DMF to afford the protect N-Boc indole **(2)**[23]. The aldehyde **(2)** was treated with CH$_3$OCH$_2$P$^+$(C$_6$H$_5$)$_3$Cl$^-$ in the presence of potassium tert-butoxide in dry THF under Wittig reaction conditions to yield intermediate **(3)**[24]. The trans (E) isomer of **3** was hydrolysed with aqueous NaOH to afford corresponding carboxylic acid **(4)**[25]. The carboxylic acid **(4)** was coupled with appropriate amine derivatives using BOP as the coupling reagent in the presence of DIPEA in DCM to obtain carboxamides **(5a-g** and **6a-f)**. Carboxamides **5a** and **5b** were cyclised by PTSA in the reflux toluene to yield the desired pyrido[3,4-b]indol-1-one products **7a** and **7b**. NMR spectroscopy and mass spectral analysis were used to determine the structures of new compounds **5a-g**, **6a-f**, **7a**, and **7b**. The presence of additional peaks in the ^{1}H and ^{13}C NMR spectra of the new compounds distinguished them from the carboxylic acid starting material **4**. In the ^{1}H NMR spectrum of **5e** (as a representative example), the disappearance of the acidic OH signal and the appearance of the amidic NH singlet signal at δ 6.60 ppm (1H) indicate amide formation. In addition, the ^{1}H NMR spectrum of **5e** revealed the characteristic signals of the methoxyvinyl group at 3-position in the form of two doublet signals of one proton each at δ 6.81 and δ 5.59 ppm corresponding to two vinyl protons (CH=CHOCH$_3$). and a singlet signal of methyl protons at 3.52 ppm (CH=CHOCH$_3$). The spectrum also showed

two signals (each of 2H) at 3.77 (q) and 2.85 (t) ppm corresponding to NCH$_2$CH$_2$ group, as well as the pyrrolidinyl protons. The ^{13}C NMR spectrum of **5e** revealed two signals at δ 41.20 and δ 34.61 ppm for (NCH$_2$CH$_2$) and (NCH$_2$CH$_2$), respectively, as well as four additional carbon signals in the aromatic. HRESI-MS with [M + H]$^+$ ion at m/z 424.1789 also validated the **5e** structure.

Biology

Antiproliferative assay
Cell viability assay. A cell viability assay was performed on the MCF-10A (human mammary gland epithelial) cell line to investigate the effect of compounds **5a-g**, **6a-f**, **7a**, and **7b** on normal cell lines[26,27]. This study employs a concentration of 50 μM of the investigated compound for four days before assessing cell viability. Compounds **5a-g**, **6a-f**, **7a**, and **7b** have no toxic effect and have greater than 87% cell viability, as shown in Table 1.

Antiproliferative assay. The newly synthesised compounds **5a-g**, **6a-f**, **7a**, and **7b** were tested for antiproliferative activity against four different types of cancer cells[28,29]: A-549 (epithelial cancer cell line), MCF-7 (breast cancer cell line), Panc-1 (pancreas cancer cell line), and HT-29 (colon cancer cell line). The results of calculating the IC$_{50}$ of each compound using erlotinib as the reference are shown in Table 1.

In general, the newly investigated compounds **5a-g**, **6a-f**, **7a**, and **7b** demonstrated promising antiproliferative activity against the four cancer cell lines tested, with mean GI$_{50}$ ranging from 29 nM to 102 nM against the four cancer cell lines when compared to the reference erlotinib, which had a GI$_{50}$ of 33 nM. The compounds with the highest antiproliferative activity were **5c**, **5d**, **5f**,
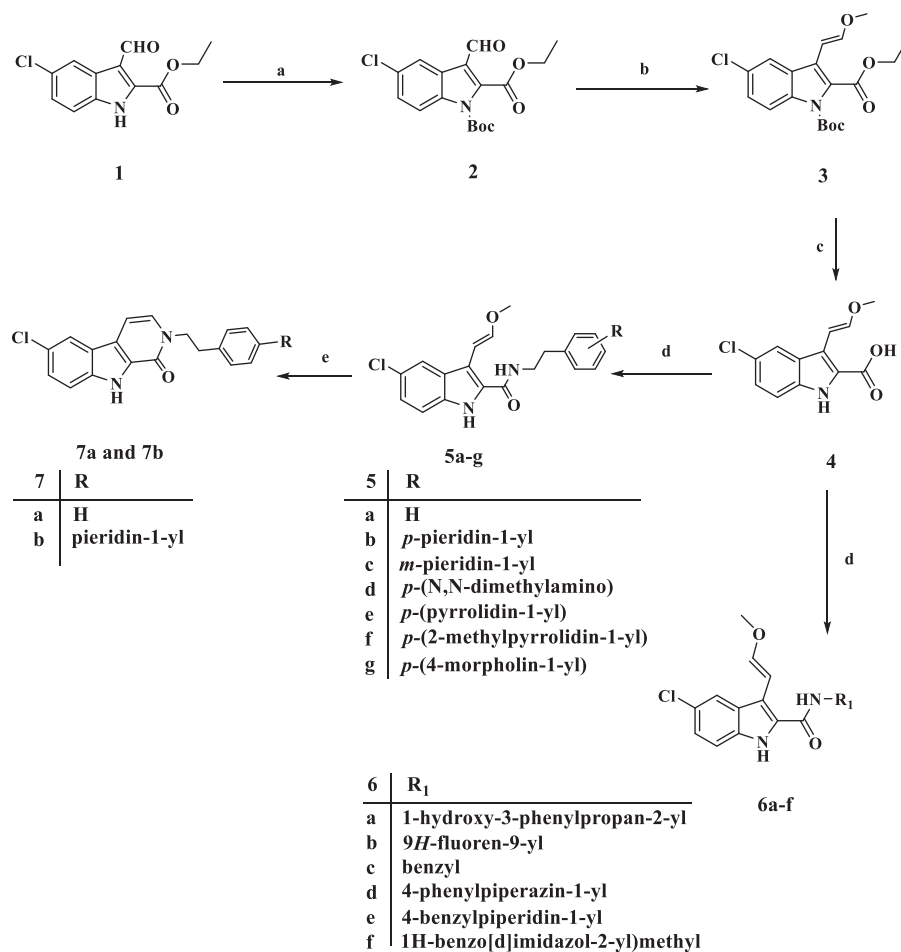
Scheme 1. Synthesis of compounds **5a-g**, **6a-f**, **7a**, and **7b**. Reagents and conditions: (a) NaH, (Boc)$_2$O, DMF, 0 °C to rt, overnight, 79%; (b) CH$_3$OCH$_2$P$^+$(C$_6$H$_5$)$_3$Cl$^-$, t-BuOK, THF, 0 °C to rt, overnight, 76%; (c) 5% NaOH, EtOH, 40 °C, 93%; (d) Amine, BOP, DIPEA, DCM, rt, overnight; (e) PTSA, toluene, reflux, overnight.

Table 1. IC$_{50}$ of compounds **5a-g**, **6a-f**, **7a**, and **7b** against four cancer cell lines.

Comp.	Cell viability %	Antiproliferative activity IC$_{50}$ ± SEM (nM)				
		A-549	MCF-7	Panc-1	HT-29	Average (GI$_{50}$)
5a	91	75 ± 8	79 ± 8	73 ± 7	75 ± 8	76
5b	89	76 ± 7	79 ± 7	75 ± 7	78 ± 7	77
5c	87	45 ± 5	49 ± 5	45 ± 5	47 ± 5	47
5d	89	34 ± 4	38 ± 3	35 ± 3	38 ± 4	36
5e	90	70 ± 7	73 ± 7	67 ± 7	71 ± 7	70
5f	87	28 ± 5	30 ± 3	27 ± 3	30 ± 3	29
5 g	89	30 ± 3	32 ± 3	30 ± 3	32 ± 3	31
6a	86	89 ± 9	92 ± 9	85 ± 9	89 ± 9	89
6b	87	102 ± 10	105 ± 10	97 ± 10	104 ± 10	102
6c	85	67 ± 6	69 ± 6	62 ± 6	64 ± 6	66
6d	89	85 ± 8	87 ± 8	81 ± 8	85 ± 8	85
6e	91	45 ± 5	47 ± 5	43 ± 4	45 ± 5	45
6f	89	40 ± 4	42 ± 4	38 ± 4	42 ± 4	41
7a	90	53 ± 5	57 ± 5	51 ± 5	55 ± 5	54
7b	89	57 ± 6	59 ± 6	55 ± 5	57 ± 6	57
Erlotinib	ND	30 ± 3	40 ± 3	30 ± 3	30 ± 3	33

ND: Not determined

5 g (Scaffold A), **6e**, and **6f** (Scaffold B), with GI$_{50}$ values ranging from 29 nM to 47 nM. With a GI$_{50}$ of 29 nM, compound **5f** (R = p-2-methyl pyrrolidin-1-yl, Scaffold A) was the most potent derivative, outperforming the reference erlotinib's GI$_{50}$ of 33 nM. Compound **5f** suppressed all cancer cell lines more efficiently than erlotinib except HT-29 (colon cancer cell line). Compounds **5 g** (R = p-4-morpholin-1-yl, Scaffold A) and **5d** (R = p-N,N-dimethyl amino,

Scaffold A) ranked second and third in activity, with GI$_{50}$ values of 31 nM and 36 nM, respectively, and were comparable to the reference erlotinib against the four tested cancer cell lines. The unsubstituted derivative, **5a** (R = H, Scaffold A), was 2.5-fold less potent than compound **5f**, whereas compounds **5b** (R = p-piperidin-1-yl, Scaffold A) and **5e** (R = p-pyrrolidin-1-yl, Scaffold A) showed moderate antiproliferative action with GI$_{50}$ values of 77 nM and 70 nM, respectively, indicating the significance of the para substitution on the phenethyl ring of compounds **5a-g**, with activity increasing in the following order: 2-methyl pyrrolidine > 4-morpholine > N,N-dimethylamine > pyrrolidine > H > piperidine.

Compound **5c** (R = m-piperidin-1-yl, Scaffold A) demonstrated good antiproliferative activity against the four tested cell lines, with a GI$_{50}$ value of 47 nM, being 1.6-fold more potent than compound **5b** (R = p-piperidin-1-yl, Scaffold A), indicating that the meta position of the phenethyl ring moiety may be tolerated for antiproliferative action than the para one. However, because only one meta-derivative (**5c**) is being prepared in the current study, this argument may require further investigation in the future.

Scaffold B compounds **6e** (R$_1$ = 4-benzylpiperidin-1-yl) and **6f** (R$_1$ = 1H-benzo[d]imidazole-2-yl)methyl) showed promising antiproliferative action with GI$_{50}$ values of 45 nM and 41 nM, respectively, approximately 1.5-fold less potent than **5c**. The remaining Scaffold B compounds **6a-d** showed moderate to weak GI$_{50}$ values ranging from 66 nM to 102 nM.

Finally, Scaffold C compounds **7a** (R$_2$ = H) and **7b** (R$_2$ = p-piperidin-1-yl) demonstrated greater antiproliferative activity

than their open-form Scaffold A counterparts **5a** and **5b**. The GI_{50} values for **7a** and **7b** were 54 nM and 57 nM, respectively, compared to 76 nM and 77 nM for **5a** and **5b**, indicating that the cyclized 1*H*-pyrido[3,4-b]indol-1-ones **7a** and **7b** are more tolerated for antiproliferative activity than the uncyclized. 3–(2-methoxyvinyl)-1H-indole-2-carboxamides **5a** and **5b**. Unfortunately, only two 1*H*-pyrido[3,4-b]indol-1-one derivatives (Scaffold C) have been synthesised. However, more Scaffold C derivatives are required to obtain a precise SAR.

EGFR inhibitory assay

The six most potent antiproliferative derivatives (**5c**, **5d**, **5f**, **5 g**, **6e**, and **6f**) were tested for inhibitory action against wild-type EGFR (EGFR^{WT})[30,31] as a potential target for their antiproliferative activity. Results are presented as IC_{50} values in Table 2. The results of this assay are consistent with those of the antiproliferative assay, in which the most potent antiproliferative derivatives, compounds **5f** (R = *p*-2-methyl pyrrolidin-1-yl, Scaffold A) and **5 g** (R = *p*-4-morpholin-1-yl, Scaffold A), were the most potent EGFR^{WT} inhibitors, with IC_{50} values of 68 ± 5 nM and 74 ± 5 nM, respectively, being more potent than the reference erlotinib ($IC_{50} = 80 \pm 5$). Compound **5d** (R = *p*-N,N-dimethylamino, Scaffold A) is the third most active compound, with an IC_{50} value of 85 ± 5, which is equivalent to erlotinib.

Compounds **5c** (R = *m*-piperidin-1-yl, Scaffold A), 6e (R_1 and $R_2 =$ 4-benzylpiperidin-1-yl, Scaffold B) and **6f** ($R_1 =$ H, $R_2 =$ 1*H*-benzo[d]imidazol-2-yl)methyl, Scaffold B) exhibited moderate anti-EGFR activity with IC_{50} values of 102 ± 7 nM, 98 ± 07 nM, and 93 ± 06, respectively being less potent than erlotinib. These findings demonstrated that compounds **5f** and **5 g** have potent EGFR^{WT} inhibitory activity and are potential antiproliferative candidates.

The inhibitory activity of the most potent compounds, **5f** and **5 g**, against mutant-type EGFR (EGFR^{T790M}) was assessed using the HTRF KinEASE-TK assay[30,31], with Osimertinib as the positive control. Compounds **5f** and **5 g**, as shown in Table 2, had excellent inhibitory activity against EGFR^{T790M}, with IC_{50} values of 9.5 ± 2 and 11.9 ± 3 nM, respectively, being equivalent to the reference osimertinib ($IC_{50} = 8 \pm 2$ nM), which may explain their potent antiproliferative activity. These findings suggested that 2-methyl pyrrolidine and morpholine substitutions in the *para*-position of the phenethyl moiety are essential for the inhibitory effect on EGFR^{T790M}.

Apoptotic marker assays

The development of novel medications that target apoptosis has become vitally important for clinical application since aberrations in apoptosis in cancer cells represent the main obstacle to the therapeutic efficacy of anticancer treatments[32]. Compounds **5f** and **5 g** were evaluated for their ability to initiate the apoptosis cascade in order to reveal their proapoptotic potential.

Table 2. IC_{50} of compounds **5c**, **5d**, **5f**, **5 g**, **6e**, and **6f** against EGFR^{WT} and EGFR^{T790M}.

Compound	EGFR^{WT} inhibition $IC_{50} \pm$ SEM (nM)	EGFR^{T790M} inhibition $IC_{50} \pm$ SEM (nM)
5c	102 ± 7	ND
5d	85 ± 5	ND
5f	68 ± 4	9.5 ± 2
5g	74 ± 5	11.9 ± 3
6e	98 ± 7	ND
6f	93 ± 6	ND
Erlotinib	80 ± 5	ND
Osimertinib	–	8 ± 2

ND: Not determined

Caspase-3 assay

Caspases have an important role in the induction and completion of apoptosis[33]. Among caspases, caspase-3 is an important caspase that cleaves various proteins in cells, resulting to apoptosis[34]. Compounds **5f** and **5 g**, the most potent derivatives, were tested as caspase-3 activators against pancreatic cancer cell line (Panc-1)[32], and the results are shown in Table 3. Compounds **5f** and **5 g** demonstrated excellent caspase-3 protein overexpression levels of 560.2 ± 5.0 and 542.5 ± 5.0 pg/mL, respectively. They increased the protein caspase-3 in the Panc-1 human pancreatic cancer cell line by approximately 8 times when compared to control untreated cells, and they were even more active than the reference staurosporine (503.2 ± 4.0 pg/mL). These results indicate that the tested compounds act as caspase-3 activators and can therefore be regarded as apoptotic inducer agents.

Caspase 8, Bax, and Bcl-2 assay

Compounds **5f** and **5 g** were further examined for their effect on caspase-8, Bax, and Bacl-2 levels against the human pancreatic cancer cell line (Panc-1)[32] using staurosporine as a reference, as presented in Table 4. The results showed that **5f** and **5 g** significantly raised the levels of caspase-8 and Bax when compared to staurosporine.

Compound **5f** had the maximum level of caspase-8 overexpression (2.10 ng/mL), followed by **5 g** (1.97 ng/mL), and reference staurosporine (1.75 ng/mL). **5f** and **5 g** elevated the caspase-8 level by 25-folds and 23-folds, respectively in comparison to the control untreated cell.

Additionally, in comparison to untreated Panc-1 cancer cells, compounds **5f** and **5 g** produced 37- and 36-fold higher levels of Bax induction (305 pg/mL and 299 pg/mL, respectively) than staurosporine (276 pg/mL, a 33-fold induction). Finally, compounds **5f** and **5 g** induced equipotent down-regulation of anti-apoptotic Bcl-2 protein levels in the Panc-1 cell line when compared to staurosporine.

Molecular modeling

The most active antiproliferative compounds (**5c**, **5d**, **5f**, **5 g**, **6e**, and **6f**) were subjected to *in silico* docking study with the aim of studying their binding modes within EGFR^{WT} active site. Molecular

Table 3. Caspase-3 level for compounds **5f**, **5 g**, and staurosporine in human pancreatic cancer cell line (Panc-1).

Compd. No.	Caspase-3	
	Conc (Pg/ml)	Fold change
5f	560.2 ± 5.0	8.5
5g	542.5 ± 5.0	8.3
Staurosporine	503.2 ± 4.0	7.6
Control	65.6	1

Table 4. Caspase-8, Bax and Bcl-2 levels for compounds **5f**, **5 g** and staurosporine on human pancreatic cancer cell line (Panc-1).

Compd. No.	Caspase-8		Bax		Bcl-2	
	Conc (ng/ml)	Fold change	Conc (Pg/ml)	Fold change	Conc (ng/ml)	Fold reduction
5f	2.10	25	305.50	37	0.80	6
5g	1.97	23	299.40	36	0.84	6
staurosporine	1.75	21	276.20	Fold reduction	0.98	5
Control	0.085	1	8.25	1	5.08	1

Table 5. Ligand-protein complex interactions of the tested compounds **5c**, **5d**, 5f, **5 g**, **6e** and 6f within the active site of EGFR^{WT}.

Compd.	MOE Score kcal/mol	Hydrogen bond interactions	Hydrophobic interactions	Other interactions
Erlotinib	−9.37	Met769 Gln767	Leu694, Leu820, Val702, Gly722, Thr766, Thr830	Lys721
5c	−8.85	Asp831	Leu694, Leu820, Asp776, Gly722, Cys773, Asp831.	————————
5d	−9.30	Met769	Leu694, Leu820, Val702, Gly722, Thr766, Pro770.	Glu738 (ionic) Leu694 (Pi-H)
5f	−9.88	Asp831 Asp776	Leu694, Leu820, Asp776, Gly722, Cys773, Asp831.	Asp776 (ionic) Cys773, Gly772 (Pi-H)
5g	−9.47	Asp831	Leu694, Leu820, Asp776, Gly722, Cys773, Asp831.	Cys773, Gly772 (Pi-H)
6e	−8.69	Asp831	Leu694, Leu820, Asp776, Gly722, Cys773, Asp831.	Cys773 (Pi-H)
6f	−9.01	Met769	Leu694, Leu820, Val702, Gly722, Thr766, Asp776, Glu780	Leu820 (Pi-H)

Operating Environment (MOE) software[35] was used along with the crystal structure of the wild-type EGFR^{WT} (PDB: 1M17)[36]. According to the prior report[37,38], ligand and protein files were prepared into the pdbqt format. The accuracy of docking simulation within the binding site of EGFR was validated via redocking the co-crystallized ligand showing *S score* of −9.37 kcal/mol with *RMSD* value of 1.39 Å, (*S1*) (Table 5). Analysis of the binding score amongst the examined compounds revealed that compounds **5f** and **5 g** showed the highest negative scores (-9.88 and −9.47 kcal/mol, respectively) comparable to the co-crystalized ligand. Binding mode analysis revealed that all compounds tested fit comfortably within the large active site. Compounds **5d**, **5f** and **5 g** with (R = *p-N,N*-dimethyl amino, *p*-2-methylpyrrolidin-1-yl and *p*-4-morpholin-1-yl moieties), respectively, exhibited better binding conformations within the binding pocket than compounds **5c**, **6e** and **6f**. Compounds **5f** and **5 g** showed almost similar binding modes. The indolyl NH of **5f** and **5 g** ligands donates an H-bond to the key amino acid Asp831 (3.25 and 3.19 Å, respectively). Also, they formed additional π-H interactions with Cys773 and Gly772 (Figure 3(A,B)). Moreover, the *p*-2-methyl pyrrolidin-1-yl moiety of compound **5f** forms an ionic bond (4.00 Å) as well as donates an H-bond (3.40 Å) to the amino acid residue Asp776 at the gate of the active site. The later interaction augments the binding pattern of compound **5f** over compound **5 g**. Both compounds exhibited comparable hydrophobic interactions and fulfilled the electrostatic interaction surface of the protein binding site (Figure 3(A,B)). Compound **5d** exhibited also good binding mode but with different orientation within the EGFR active site. Compound **5d** extends deeply into the hydrophobic pocket with its *p-N,N*-dimethylamino phenyl moiety forming ionic interaction with Glu738 (3.69 Å). The complex also is stabilised by accepting H-bond interaction from the key amino acid Met769 (2.84 Å) residue to the ligand amidic carbonyl group. In addition, the ligand forms pi-H interaction with Leu694 from the 5-chloro-indolyl moiety which projects parallel to the erlotinib ether chain. Compounds **5c** and **6e** resemble compounds **5f** and **5 g** in their binding modes, however losing interaction with Asp766 at the opening of the active site. Furthermore, compound **6f** probes the space of the active site in an analogous pattern to that of compound **5d** while missing interaction with the amino acid residue Glu738 at the hydrophobic pocket. Other ligands interactions within the active site include hydrophobic ones with Leu694, Leu820, Val702, Gly722, Thr766 and Phe771.

The most potent compounds **5f** and **5 g** were further subjected to a docking study within the active pocket of the EGFR mutant type T790M for a deep understanding of their inhibition mode using the crystal structure of protein entry (PDB: 5J9Z)[39] for a deep understanding of their inhibition mode. The docking protocol was validated by redocking the co-crystallized ligand that exhibited S score of −10.42 kcal/mol with RMSD value of 0.88 Å, (*S2*). Compounds **5f** and **5 g** showed good negative scores (–9.43 and −9.31 kcal/mol) (Table 6) comparable to the co-crystalized ligand although they did not bind in a covalent fashion. The ligand 5-chloro-indolyl moiety is inserted deeply inside the hydrophobic pocket where the indolyl NH donates an H-bond interaction to the amino acid Asp855 (2.99 and 3.01 Å). Also, their quaternary amine moieties form ionic bonds (2.98 and 2.94 Å) as well as H-bond interactions with Asp800 (3.31 and 3.17 Å) at the gate of the binding site. Moreover, the compounds formed additional π-H and π-cation interactions with Leu844 and Lys745, respectively, although they missed interactions with Met790, Gln791 and Met793 amino acid residues at the hydrophobic pocket. (Figure 3(C,D)). They exhibited comparable hydrophobic interactions with Asp800, Phe723, Leu844, Cys797, Leu718, Val726, Met790, Lys745 that strengthen the stability of the complexes within the protein binding site. The docking simulations tried to examine the binding mode of the most active compounds within the binding site of wild-type EGFR as well as EGFR mutant type T790M and confirmed the dual inhibitory effects of compounds **5f** and **5 g**.

In silico *ADME/pharmacokinetics studies*

The most potent compounds **5f and 5 g** were subjected to *in silico* ADME studies using the web tool SwissADME[40] by entering a list of two compounds' SMILES (Simplified Molecule Input Line Entry Specification) provided by ChemDraw software. The *in silico* pharmacokinetic data (Table 7) showed that both compounds are orally active as they obey Lipinski's rules of five with zero violation. Both compounds are actively effluxed by P-gp and exhibit high intestinal absorbance. Also, both compounds are capable to cross BBB. Drug permeability is a significant parameter that predicts the destiny of a drug. Based on Lipinski's rules, it should be ≤ 5. Both compounds exhibited good permeability as indicated by logP values of 4.68 and 3.83. Only compound **5f** is likely to be metabolised by CYP1A2 while both compounds are going to be CYP2D6, CYP3A4, CYP2C19 and CYP2C9 inhibitors. The results predict that both compounds exhibit good Pharmacokinetics and ADME properties (Tables 7 and 8).

Conclusion

A new series of 5-chloro-3–(2-methoxyvinyl)-indole-2-carboxamide and pyrido[3,4-b] Indol-1-one derivatives were synthesised and
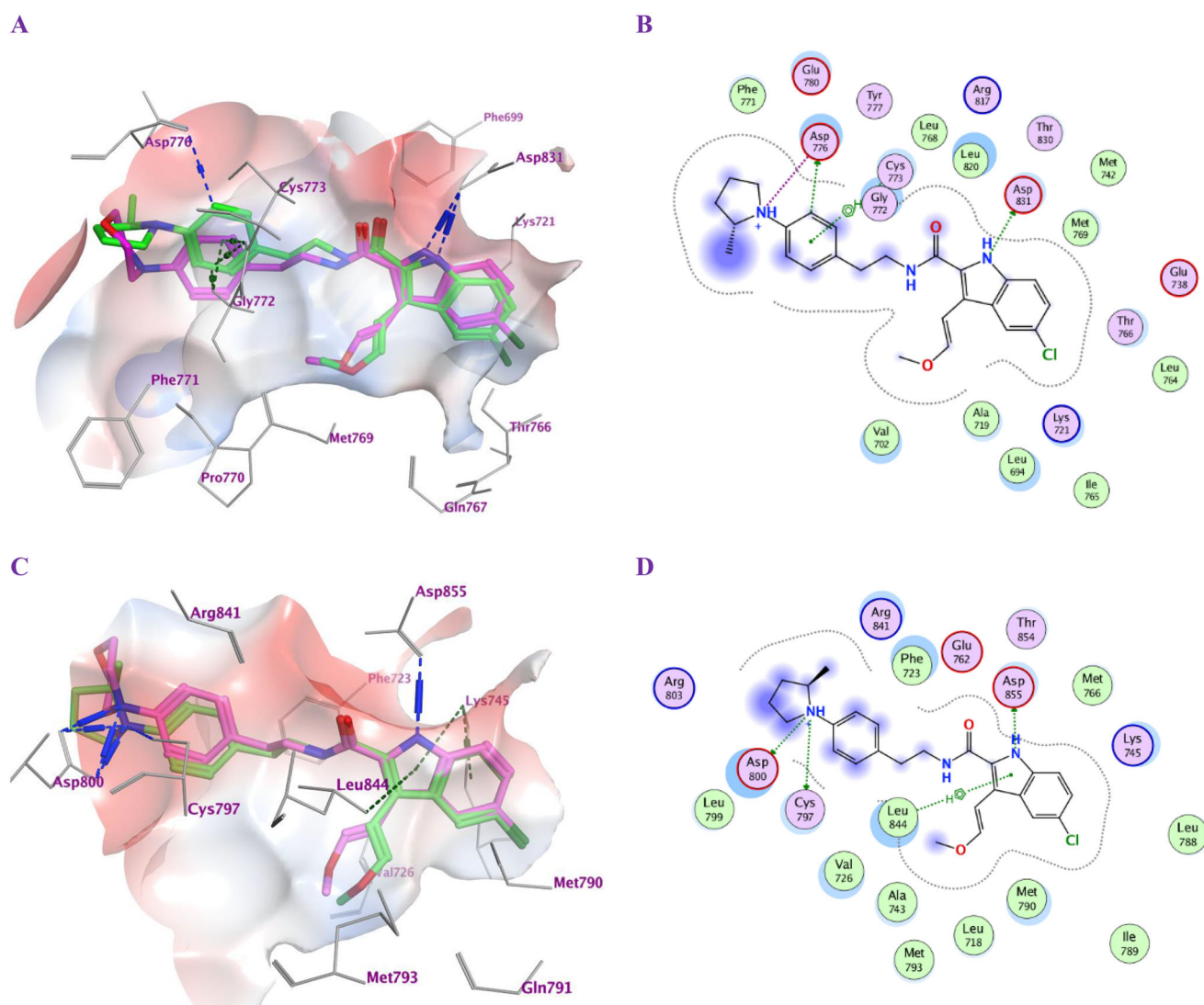
Figure 3. Docking representation models for compounds **5f** and **5 g**; (A) 3D-docked models of compound **5f** (green) aligned with **5 g** (purple) within the active site of EGFR^WT showing the interaction surface of the protein (electrostatics; green: hydrophobic, blue; positive and red: negative); (B) 2D-docked model of compound **5f** within the active site of EGFR^WT; (C) 3D-docked models of compound **5f** (green) aligned with **5 g** (purple) within the active site of EGFR^T790M showing the interaction surface of the protein (electrostatics; green: hydrophobic, blue; positive and red: negative); (D) 2D-docked model of compound **5f** within the active site of EGFR^T790M.

Table 6. Ligand-protein complex interactions of the tested compounds **5f** and **5 g** within the active site of EGFR^T790M.

Compd.	MOE Score kcal/mol	Hydrogen bond interactions	Hydrophobic interactions	Other interactions
Co-crystalized ligand (6HJ)[a]	−10.42	Met790 Gln791 Met793	Leu844, Cys797, Leu718, Val726, Met790	Val726 (Pi-H) Cys797 (covalent)
5f	−9.43	Asp855 Cys797 Asp800	Asp800, Phe723, Leu844, Cys797, Leu718, Val726, Met790, Lys745.	Asp800 (Ionic) Leu844 (Pi-H)
5g	−9.31	Asp855 Asp800	Asp800, Phe723, Leu844, Cys797, Leu718, Val726, Met790	Asp800 (Ionic) Lys745 (Pi-cation) Leu844 (Pi-H)

[a] (R)-1–(3-(4-amino-3–(1-methyl-1H-indol-3-yl)-1H-pyrazolo[3,4-d]pyrimidin-1-yl)piperidin-1-yl)prop-2-en-1-one.

Table 7. Physicochemical and pharmacokinetic properties (*Lipinski parameters*) of compounds **5f and 5 g**.

Compd.	MW	^{n}ROTB	HBA	HBD	Violations	MR	TPSA	Log P
5f	438	8	2	2	0	131.03	57.36	4.68
5g	440	8	3	2	0	127.31	66.59	3.83

structurally characterised utilising several spectroscopic methods of analysis. The compounds had no cytotoxic effects on normal cell lines but showed promising antiproliferative properties against

four human cancer cell lines. Some of the compounds tested showed potent inhibitory activity against both wild-type and mutant-type EGFR, as well as apoptotic-inducing activity. *In silico* docking studies attempted to explore the binding mode of the most active antiproliferative compounds within the binding site of EGFR^WT-TK. Results proved the best binding modes for compounds **5f** and **5 g** that confirmed their highest potency compared to erlotinib. Also, docking results of both compounds against EGFR^T790M conclude that addressing the hydrophobic

Table 8. ADME properties of compounds **5f and 5 g**.

Compd.	GI Abs.	BBB	P-gp substrate	CYP1A2 inhibitor	CYP2C19 inhibitor	CYP2C9 inhibitor	CYP2D6 inhibitor	CYP3A4 inhibitor
5f	High	Yes	Yes	No	Yes	Yes	Yes	Yes
5g	High	Yes	Yes	Yes	Yes	Yes	Yes	Yes

pocket that comprises the Met790 amino acid with lipophilic scaffold may explain their affinity owing to reduced interactions with the polar Thr790 in EGFR^{WT}. *In silico* ADME and pharmacokinetic prediction validated that the most potent compounds **5f** and **5 g** have good bioavailability and pharmacokinetic profiles. After structural modifications, **5f** and **5 g** may act as anticancer agents targeting EGFR^{T790M}, but more *in vitro* and *in vivo* testing is required.

Experimental

General details: See Appendix A (Supplementary File)

Chemistry

Synthesis of 1-tert-butyl 2-ethyl 5-chloro-3-formyl-1H-indole-1,2-dicarboxylate (2)

A solution of indole ester **1** (1 g, 3.97 mmol) in DMF (0.2 M) was added dropwise at 0 °C to a suspension of NaH (0.25 g, 5.96 mmol, 60% dispersion in mineral oil) in DMF (0.2 M). After stirring 0.5 h, the resulting mixture was treated dropwise with (Boc)$_2$O (1.34 g, 5.96 mmol). The cooling bath was removed, and the mixture was stirred overnight at rt. The reaction mixture was diluted with EtOAc and successively washed twice with water. EtOAc layer was washed with brine, dried over MgSO$_4$, and concentrated under reduced pressure to yield compound **2** (1.1 g, 71%) as a white solid after purification by flash chromatography on silica gel using a mixture of EtOAc, hexanes (1:10) as eluent; mp 58–59 °C.

ν $_{max}$ (KBr disc)/cm^{-1} 2983, 2939, 2872, 1750 (C=O), 1721 (C=O), 1670 (C=O), 1555, 1443, 1384, 1225, 1150, 840, 802, 764, 697. ^{1}H NMR (250 MHz, CDCl$_3$): δ 10.11 (1H, s, CHO); 8.29 (1H, s); 7.95 (1H, d, J = 8.8 Hz); 7.39 (1H, d, J = 9.3 Hz); 4.49 (2H, q, J = 7.0 Hz); 1.60 (9H, s); 1.43 (3H, t, J = 7.0 Hz). ^{13}C NMR (62.5 MHz, CDCl$_3$): δ (62.5 MHz, CDCl$_3$): δ 185.6; 160.7; 147.9; 138.9; 133.9; 131.1; 127.7; 125.8; 122.5; 119.9; 116.0; 87.2; 63.0; 27.8; 14.2. HRESI-MS m/z calcd for [M + H]$^+$ C$_{17}$H$_{19}$ClNO$_5$: 352.0946, found: 352.0950.

Synthesis of (E)-1-tert-butyl 2-ethyl 5-chloro-3–(2-methoxyvinyl)-1H-indole-1,2-dicarboxylate (3)

To a stirred suspension of CH$_3$OCH$_2$P$^+$(C$_6$H$_5$)$_3$Cl$^-$ (2.17 g, 3 equiv) in anhydrous THF (20 ml) at 0 °C under N$_2$ atmosphere, *t*-BuOK (2.17 g, 3 equiv) was added. The resulting mixture was stirred for additional 10 min at 0 °C before treating dropwise with a solution of **2** (0.74 g, 2.10 mmol, 1 equiv) in THF (20 ml). The cooling bath was removed, and the mixture was stirred overnight at rt. After concentration of the solvent *in vacuo*, the residue was taken up in EtOAc, washed with saturated solution of NaHCO$_3$, brine, dried over MgSO$_4$, and concentrated under reduced pressure. Flash chromatography of the crude product using (1:10) EtOAc/hexanes provided **3** (*E*) (0.53 g, 66%) as a white solid; mp 98–99 °C which was used for alkaline hydrolysis step and *cis* (*Z*) isomer (0.12 g, 15%) as a yellow oil.

Compound 3 (*E*): ν $_{max}$ (KBr disc)/cm^{-1} 2981, 2935, 1729 (C=O), 1710 (C=O), 1635 (C=C), 1532, 1447, 1353, 1209, 1123, 1123, 962, 827, 777, 642. ^{1}H NMR (250 MHz, CDCl$_3$): δ 8.00 (1H, d, J = 6.3 Hz); 7.65 (1H, s); 7.32 (1H, d, J = 9.3 Hz); 7.23 (1H, d, J = 13.5 Hz); 5.98 (1H, d, J = 13.3 Hz); 4.34 (2H, q, J = 7.0 Hz); 3.68 (3H, s); 1.60 (9H, s); 1.34 (3H, t, J = 7.0 Hz). ^{13}C NMR (62.5 MHz, CDCl$_3$): δ 162.5; 152.5; 149.1; 135.2; 128.9; 128.3; 126.9; 121.1; 120.7; 116.3; 94.5; 84.9; 61.5; 56.5; 53.5; 27.9; 14.2. HRESI-MS m/z calcd for [M + H]$^+$ C$_{19}$H$_{23}$ClNO$_5$: 380.1259, found: 380.1261.

Synthesis of (E)-5-Chloro-3–(2-methoxyvinyl)-1H-indole-2-carboxylic acid (4)

To a solution of compound **3** (trans isomer) (0.67 g, 1.76 mmol) in ethanol, (0.5 M), 5% NaOH (9 ml, 5 equiv) was added. The reaction mixture was kept at 40 °C with stirring overnight. The residue after removal of ethanol under reduced pressure was then taken into water, precipitated out at pH = 1 using 5% HCl and the precipitate extracted with EtOAc, dried over MgSO$_4$, and evaporated under reduced pressure to afford **4** (0.41 g, 93%) as a pale-yellow solid; mp 132–134 °C.

ν $_{max}$ (KBr disc)/cm^{-1} 33427 (NH), 3100 (br, OH), 2941, 1680 (C=O), 1643 (C=C), 1529, 1448, 1333, 1256, 1114, 929, 814, 796, 778. ^{1}H NMR (250 MHz, CD$_3$OD): δ 7.78 (1H, s); 7.48–7.10 (3H, m); 6.65 (1H, d, J = 13.3 Hz); 3.76 (3H, s). ^{13}C NMR (62.5 MHz, CD$_3$OD): δ 163.5; 149.8; 135.1; 125.6; 125.2; 124.9; 123.6; 120.5; 118.1; 113.2; 98.0; 55.2. HRESI-MS m/z calcd for [M + H]$^+$ C$_{12}$H$_{11}$ClNO$_3$: 252.0422, found: 252.0425.

Synthesis of compounds 5a-g and 6a-f

A mixture of indole-2-carboxylic acid **4** (0.52 mmol), BOP (0.34 g, 0.77 mmol), and DIPEA (0.17 ml, 1.03 mmol) in DCM (0.05 M) was stirred for 10 min at rt before addition of the appropriate amine (0.62 mmol), and the resulting reaction mixture was stirred overnight at rt. After removing of the solvent *in vacuo*, the residue was extracted with EtOAc, washed with 5% HCl, saturated NaHCO$_3$ solution, brine, dried over MgSO$_4$, and evaporated under reduced pressure to give a crude product which was purified by flash chromatography on silica gel using a mixture of EtOAc, hexanes (1:2) as an eluent.

(E)-5-Chloro-3–(2-methoxyvinyl)-N-phenethyl-1H-indole-2-carboxamide (5a).
Yield 76%; mp 150–152 °C; ν $_{max}$ (KBr disc)/cm^{-1} 3257 (NH), 2950, 1650 (C=O), 1622 (C=C), 1637, 1451, 1218, 1163, 960, 801, 700; ^{1}H NMR (250 MHz, CDCl$_3$): δ 9.84 (s br, 1H, indole NH), 7.58 (s, 1H, Ar-H), 7.56–7.19 (m, 7H, Ar-H), 6.77 (d, J = 13.00 Hz, 1H, CH=CHOCH$_3$), 6.59 (s br, 1H, amide NH), 5.54 (d, J = 13.00 Hz, 1H, CH=CHOCH$_3$), 3.81 (q, J = 6.25 Hz, 2H, NHCH$_2$CH$_2$), 3.52 (s, 3H, OCH$_3$), 2.95 (t, J = 6.25 Hz, 2H, NHCH$_2$CH$_2$); ^{13}C NMR (62.5 MHz, CDCl$_3$): δ 162.01 (C=O), 153.41, 138.75, 133.67, 128.94, 128.83, 128.11, 126.72, 126.03, 125.13, 120.04, 113.08, 111.31, 93.37, 56.71, 40.84, 35.64; HRESI-MS m/z calcd for [M + H]+ C$_{20}$H$_{20}$ClN$_2$O$_2$: 355.1208, found: 355.1211.

(E)-5-chloro-3–(2-methoxyvinyl)-N-(4-(piperidin-1-yl)phenethyl)-1H-indole-2-carboxamide (5b).
Yield 81%; mp 170–172 °C; ν $_{max}$ (KBr disc)/cm^{-1} 3378 (NH), 3228 (NH), 2929, 2845, 1634 (C=O), 1620 (C=C), 1540, 1451, 1326, 1214, 1162, 1130, 959, 863, 804, 777, 693; ^{1}H NMR (400 MHz, Chloroform-*d*) δ 9.66 (s, 1H, indole NH),

7.59 (d, $J = 2.0$ Hz, 1H, Ar-H), 7.33 (d, $J = 8.7$ Hz, 1H, Ar-H), 7.21 (dd, $J = 8.7$, 2.0 Hz, 1H, Ar-H), 7.11 (d, $J = 8.9$ Hz, 2H, Ar-H), 6.89 (d, $J = 8.6$ Hz, 2H, Ar-H), 6.79 (d, $J = 13.0$ Hz, 1H, CH=CHOCH$_3$), 6.58 (t, $J = 5.8$ Hz, 1H, amide NH), 5.59 (d, $J = 13.0$ Hz, 1H, CH=CHOCH$_3$), 3.76 (q, $J = 6.5$ Hz, 2H, NHCH$_2$CH$_2$), 3.56 (s, 3H, OCH$_3$), 3.16–3.08 (m, 4H, piperidin-H), 2.86 (t, $J = 6.6$ Hz, 2H, NHCH$_2$CH$_2$), 1.76–1.65 (m, 4H, piperidin-H), 1.63–1.52 (m, 2H, piperidin-H); ^{13}C NMR (101 MHz, cdcl$_3$) δ 161.86, 153.29, 151.07, 133.57, 129.28, 128.90, 128.85, 128.21, 125.96, 125.02, 119.98, 116.76, 112.98, 111.20, 93.42, 56.67, 50.67, 40.93, 34.63, 25.89, 24.27; HRESI-MS m/z calcd for [M + H]$^+$ C$_{25}$H$_{29}$ClN$_3$O$_2$: 438.1943, found: 438.1943.

(E)-5-chloro-3–(2-methoxyvinyl)-N-(3-(piperidin-1-yl)phenethyl)-1H-indole-2-carboxamide (5c).
Yield 86%; mp 80–82 °C; ^{1}H NMR (400 MHz, CDCl$_3$) δ 10.05 (s, 1H, indole NH), 7.59 (d, $J = 2.0$ Hz, 1H, Ar-H), 7.36 (d, $J = 8.7$ Hz, 1H, Ar-H), 7.25–7.15 (m, 2H, Ar-H), 6.85–6.75 (m, 3H, Ar-H, CH=CHOCH$_3$), 6.70 (d, $J = 7.5$ Hz, 1H, Ar-H), 6.66 (s, 1H, amide NH), 5.59 (d, $J = 13.0$ Hz, 1H, CH=CHOCH$_3$), 3.81 (q, $J = 6.7$ Hz, 2H, NHCH$_2$), 3.55 (s, 3H, OCH$_3$), 3.15–3.08 (m, 4H, piperidin-H), 2.91 (t, $J = 6.7$ Hz, 2H, NHCH$_2$CH$_2$), 1.71–1.61 (m, 4H, piperidin-H), 1.60–1.50 (m, 2H, piperidin-H); ^{13}C NMR (101 MHz, CDCl$_3$) δ 162.08 (C=O), 153.26, 152.61, 139.40, 133.79, 129.36, 128.80, 128.12, 125.91, 125.02, 119.96, 119.30, 116.77, 114.59, 113.10, 111.37, 93.44, 56.64, 50.46, 40.87, 35.95, 25.80, 24.25; HRESI-MS m/z calcd for [M + H]$^+$ C$_{25}$H$_{29}$ClN$_3$O$_2$: 438.1943, found: 438.1944.

(E)-5-chloro-N-(4-(dimethylamino)phenethyl)-3-(2-methoxyvinyl)-1H-indole-2-carboxamide (5d).
Yield 82%; mp 177–179 °C; ^{1}H NMR (400 MHz, CDCl$_3$) δ 9.72 (s, 1H, indole NH), 7.59 (s, 1H, Ar-H), 7.34 (d, $J = 8.7$, Hz, 1H. Ar-H), 7.21 (dd, $J = 8.7$, 2.0 Hz, 1H, Ar-H), 7.11 (d, $J = 8.5$ Hz, 2H, Ar-H), 6.80 (d, $J = 13.0$ Hz, 1H, CH=CHOCH$_3$), 6.71 (d, $J = 8.5$ Hz, 2H, Ar-H), 6.59 (s, 1H, amide NH), 5.58 (d, $J = 13.0$ Hz, 1H, CH=CHOCH$_3$), 3.76 (q, $J = 66$ Hz, 2H, NHCH$_2$), 3.53 (s, 3H, OCH$_3$), 2.93 (s, 6H, N(CH$_3$)$_2$), 2.85 (t, $J = 6.6$ Hz, 2H, NHCH$_2$CH$_2$); ^{13}C NMR (101 MHz, CDCl$_3$) δ 161.87 (C=O), 153.27, 149.52, 133.60, 129.37, 128.88, 128.23, 126.26, 125.95, 125.00, 119.97, 113.02, 113.00, 111.22, 93.40, 56.56, 41.04, 40.68, 34.53; HRESI-MS m/z calcd for [M + H]$^+$ C$_{22}$H$_{25}$ClN$_3$O$_2$: 398.1630, found: 398.1628.

(E)-5-chloro-3-(2-methoxyvinyl)-N-(4-(pyrrolidin-1-yl)phenethyl)-1H-indole-2-carboxamide (5e).
Yield 83%; mp 185 - 187 °C; ^{1}H NMR (400 MHz, CDCl$_3$) δ 9.97 (s, 1H, indole NH), 7.59 (s, 1H, Ar-H), 7.35 (d, $J = 8.7$ Hz, 1H, Ar-H), 7.21 (dd, $J = 8.7$, 2.0 Hz, 1H, Ar-H), 7.09 (d, $J = 8.4$ Hz, 2H, Ar-H), 6.81 (d, $J = 13.0$ Hz, 1H, CH=CHOCH$_3$), 6.60 (s, 1H, amide NH), 6.53 (d, $J = 8.4$ Hz, 2H, Ar-H), 5.59 (d, $J = 13.0$ Hz, 1H, CH=CHOCH$_3$), 3.77 (q, $J = 6.4$ Hz, 2H, NHCH$_2$), 3.52 (s, 3H, OCH$_3$), 3.30–3.22 (m, 4H, pyrrolidin-H), 2.85 (t, $J = 6.6$ Hz, 2H, NHCH$_2$CH$_2$), 2.05–1.96 (m, 4H, pyrrolidin-H); ^{13}C NMR (101 MHz, CDCl$_3$) δ 161.95 (C=O), 153.21, 146.85, 133.72, 129.44, 128.81, 128.28, 125.88, 124.93, 124.87, 119.93, 113.09, 111.94, 111.20, 93.47, 56.53, 47.64, 41.20, 34.61, 25.47; HRESI-MS m/z calcd for [M + H]$^+$ C$_{24}$H$_{27}$ClN$_3$O$_2$: 424.1786, found: 424.1789.

(E)-5-chloro-3-(2-methoxyvinyl)-N-(4-(2-methylpyrrolidin-1-yl)phenethyl)-1H-indole-2-carboxamide (5f).
Yield 85%; mp 151–153 °C; ^{1}H NMR (400 MHz, CDCl$_3$) δ 9.64 (s, 1H, indole NH), 7.59 (s 1H, Ar-H), 7.34 (d, $J = 8.8$ Hz, 1H, Ar-H), 7.21 (dd, $J = 8.7$, 2.0 Hz, 1H, Ar-H), 7.08 (d, $J = 8.4$ Hz, 2H, Ar-H), 6.81 (d, $J = 13.0$ Hz, 1H, CH=CHOCH$_3$), 6.62–6.51 (m, 3H, amide NH, Ar-H), 5.59 (d, $J = 13.0$ Hz, 1H, CH=CHOCH$_3$), 3.88–3.70 (m, 3H, pyrrolidin-H, NHCH$_2$), 3.52 (s, 3H, OCH$_3$), 3.41 (dd, $J = 9.4$, 7.3 Hz, 1H, pyrrolidin-H), 3.13 (m, 1H,

pyrrolidin-H), 2.83 (t, $J = 6.6$ Hz, 2H, NHCH$_2$CH$_2$), 2.13–1.93 (m, 3H, pyrrolidin-H), 1.71 (m, 1H, pyrrolidin-H), 1.17 (d, $J = 6.2$ Hz, 3H, CHCH$_3$); ^{13}C NMR (101 MHz, CDCl$_3$) δ 161.82 (C=O), 153.24, 146.10, 133.56, 129.48, 128.87, 128.28, 125.93, 124.97, 124.66, 119.98, 112.97, 112.00, 111.19, 93.37, 56.48, 53.68, 48.27, 41.13, 34.55, 33.12, 23.31, 19.43; HRESI-MS m/z calcd for [M + H]$^+$ C$_{25}$H$_{29}$ClN$_3$O$_2$: 438.1943, found: 438.1941.

(E)-5-chloro-3-(2-methoxyvinyl)-N-(4-morpholinophenethyl)-1H-indole-2-carboxamide (5 g).
Yield 87%; mp 180–182 °C; ^{1}H NMR (400 MHz, DMSO-d$_6$) δ 11.50 (s, 1H, indole NH), 7.90 (t, $J = 5.6$ Hz, 1H, amide NH), 7.74 (s, 1H, Ar-H), 7.40 (d, $J = 8.7$ Hz, 1H, Ar-H), 7.24–7.15 (m, 2H, Ar-H, CH=CHOCH$_3$), 7.10 (d, $J = 8.6$ Hz, 2H, Ar-H), 6.85 (d, $J = 8.6$ Hz, 2H, Ar-H), 6.33 (d, $J = 13.2$ Hz, 1H, CH=CHOCH$_3$), 3.73–3.66 (m, 4H, morph-H), 3.63 (s, 3H, OCH$_3$), 3.48 (q, $J = 7.8$ Hz, 2H, NHCH$_2$), 3.06–2.98 (m, 4H, morph-H), 2.76 (t, $J = 7.3$ Hz, 2H, NHCH$_2$CH$_2$); ^{13}C NMR (101 MHz, DMSO-d$_6$) δ 161.87 (C=O), 150.14, 149.96, 134.58, 130.36, 129.58, 128.80, 126.50, 124.82, 124.30, 120.57, 115.70, 114.20, 113.14, 97.73, 66.57, 56.68, 49.13, 41.26, 34.63; HRESI-MS m/z calcd for [M + H]$^+$ C$_{24}$H$_{27}$ClN$_3$O$_3$: 440.1735, found: 440.1737.

(E)-5-chloro-N-(1-hydroxy-3-phenylpropan-2-yl)-3-(2-methoxyvinyl)-1H-indole-2-carboxamide (6a).
Yield 80%; mp 152–154 °C; ^{1}H NMR (400 MHz, CDCl$_3$) δ 9.41 (s, 1H, indole NH), 7.58 (s, 1H, Ar-H), 7.35–7.18 (m, 7H, Ar-H), 6.93 (d, $J = 7.8$ Hz, 1H, Ar-H), 6.82 (d, $J = 13.0$ Hz, 1H, CH=CHOCH$_3$), 5.67 (d, $J = 13.0$ Hz, 1H, CH=CHOCH$_3$), 4.44–4.40 (m, 1H, NHCH), 3.86–3.71 (m, 2H, CH$_2$OH), 3.68 (s, 3H, OCH$_3$), 3.01 (d, $J = 7.1$ Hz, 2H, CHCH$_2$), 2.56 (t, $J = 5.3$ Hz, 1H, OH); ^{13}C NMR (101 MHz, CDCl$_3$) δ 162.19 (C=O), 153.47, 137.42, 133.58, 129.20, 128.82, 128.73, 127.75, 126.80, 126.12, 125.29, 120.08, 112.93, 111.93, 93.43, 64.06, 56.67, 53.09, 37.17; HRESI-MS m/z calcd for [M + H]$^+$ C$_{21}$H$_{22}$ClN$_2$O$_3$: 385.1313, found: 385.1313.

(E)-5-chloro-N-(9H-fluoren-9-yl)-3-(2-methoxyvinyl)-1H-indole-2-carboxamide (6b).
Yield 86%; mp 240–241 °C; ^{1}H NMR (400 MHz, DMSO-d$_6$) δ 11.46 (s, 1H, indole NH), 8.59 (d, $J = 8.2$ Hz, 1H, amide NH), 7.88 (d, $J = 7.6$ Hz, 2H, Ar-H), 7.81 (d, $J = 2.0$ Hz, 1H, Ar-H), 7.61 (q, $J = 7.5$ Hz, 2H, Ar-H), 7.48–7.32 (m, 5H, Ar-H), 7.28 (d, $J = 13.3$ Hz, 1H, CH=CHOCH$_3$), 7.21 (dd, $J = 8.7$, 2.0 Hz, 1H, Ar-H), 6.65 (d, $J = 13.3$ Hz, 1H, CH=CHOCH$_3$), 6.25 (d, $J = 8.1$ Hz, 1H, NHCH), 3.66 (s, 3H, OCH$_3$); ^{13}C NMR (101 MHz, DMSO-d$_6$) δ 162.73 (C=O), 149.92, 145.08, 140.63, 134.74, 128.94, 128.12, 127.76, 126.13, 125.50, 124.91, 124.62, 120.84, 120.66, 114.91, 114.21, 98.52, 56.61, 54.85; HRESI-MS m/z calcd for [M + H]$^+$ C$_{25}$H$_{20}$ClN$_2$O$_2$: 415.1208, found: 415.1209.

(E)-N-benzyl-5-chloro-3-(2-methoxyvinyl)-1H-indole-2-carboxamide (6c).
Yield 82%; mp 170–172 °C; ^{1}H NMR (400 MHz, CDCl$_3$) δ 9.82 (s, 1H, indole NH), 7.60 (d, $J = 2.0$, Hz, 1H, Ar-H), 7.41–7.16 (m, 7H, Ar-H), 6.95 (s, 1H, amide NH), 6.85 (d, $J = 13.0$ Hz, 1H, CH=CHOCH$_3$), 5.81 (d, $J = 13.0$ Hz, 1H, CH=CHOCH$_3$), 4.71 (d, $J = 5.7$ Hz, 2H, NHCH$_2$), 3.63 (s, 3H, OCH$_3$); ^{13}C NMR (101 MHz, CDCl$_3$) δ 161.99 (C=O), 153.45, 137.85, 133.73, 128.86, 128.85, 127.91, 127.71, 127.58, 126.06, 125.20, 120.00, 113.09, 111.53, 93.80, 56.75, 43.85; HRESI-MS m/z calcd for [M + H]$^+$ C$_{19}$H$_{18}$ClN$_2$O$_2$: 341.1051, found: 341.1053.

(E)-(5-chloro-3–(2-methoxyvinyl)-1H-indol-2-yl)(4-phenylpiperazin-1-yl) methanone (6d).
Yield 78%; mp 102–104 °C; ^{1}H NMR (400 MHz, CDCl$_3$) δ 9.98 (s, 1H, indole NH), 7.68 (d, $J = 2.0$ Hz, 1H,

Ar-H), 7.33–7.23 (m, 3H, Ar-H), 7.21–7.14 (m, 1H, Ar-H), 7.00 (d, $J = 13.0$ Hz, 1H, CH=CHOCH$_3$), 6.96–6.86 (m, 3H, Ar-H), 5.87 (d, $J = 13.0$ Hz, 1H, CH=CHOCH$_3$), 3.81 (t, $J = 6.5$ Hz, 4H, piperazin-H), 3.72 (s, 3H, OCH$_3$), 3.16 (t, $J = 5.2$ Hz, 4H, piperazin-H); ^{13}C NMR (101 MHz, CDCl$_3$) δ 164.47 (C=O), 150.75, 150.13, 134.78, 129.29, 126.91, 126.50, 125.92, 124.40, 120.71, 119.96, 116.74, 113.07, 111.86, 96.45, 56.88, 49.74; HRESI-MS m/z calcd for [M + H]$^+$ C$_{22}$H$_{23}$ClN$_3$O$_2$: 396.1473, found: 396.1474.

(E)-(4-benzylpiperidin-1-yl)(5-chloro-3–(2-methoxyvinyl)-1H-indol-2-yl) methanone (6e).
Yield 79%; mp 95–97 °C; ^{1}H NMR (400 MHz, CDCl$_3$) δ 9.74 (s, 1H, indole NH), 7.65 (s, 1H, Ar-H), 7.33–7.07 (m, 7H, Ar-H), 6.96 (d, $J = 13.0$ Hz, 1H, CH=CHOCH$_3$), 5.82 (d, $J = 13.0$ Hz, 1H, CH=CHOCH$_3$), 3.72 (s, 3H, OCH$_3$), 2.89–2.85 (m, 2H, piperidin-H), 2.53 (d, $J = 7.0$ Hz, 2H, CHCH$_2$), 1.84–1.65 (m, 4H, piperidin-H), 1.31–1.14 (m, 3H, piperidin-H); ^{13}C NMR (101 MHz, CDCl$_3$) δ 164.17 (C=O), 149.75, 139.73, 134.60, 129.05, 128.32, 127.61, 126.53, 126.10, 125.77, 124.09, 119.84, 112.93, 111.31, 96.61, 56.82, 42.86, 38.16, 32.27; HRESI-MS m/z calcd for [M + H]$^+$ C$_{24}$H$_{26}$ClN$_2$O$_2$: 409.1677, found: 409.1678.

(E)-N-((1H-benzo[d]imidazol-2-yl)methyl)-5-chloro-3–(2-methoxyvinyl)-1H-indole-2-carboxamide (6f).
Yield 80%; mp 205–207 °C; ^{1}H NMR (400 MHz, DMSO-d$_6$) δ 12.33 (s, 1H, indole NH), 11.60 (s, 1H, imidazol NH), 8.52 (t, $J = 5.6$ Hz, 1H, amide NH), 7.79 (s, 1H, Ar-H), 7.53–7.40 (m, 3H, Ar-H), 7.31–7.19 (m, 1H, Ar-H), 7.16– 7.12 (m, 2H, Ar-H), 6.54 (d, $J = 13.2$ Hz, 1H, CH=CHOCH$_3$), 4.74 (d, $J = 5.6$ Hz, 2H, NHCH$_2$), 3.70 (s, 3H, OCH$_3$); ^{13}C NMR (101 MHz, DMSO-d$_6$) δ 162.11 (C=O), 152.47, 150.45, 134.76, 128.08, 126.44, 124.92, 124.60, 121.94, 120.74, 114.28, 114.17, 97.79, 56.65, 38.01; HRESI-MS m/z calcd for [M + H]$^+$ C$_{20}$H$_{18}$ClN$_4$O$_2$: 381.1113, found: 381.1113.

Synthesis of compounds 7a and 7b
A mixture of **5a or 5b** (0.32 mmol, 1 equiv) and PTSA (0.03 g, 0.5 equiv) in toluene (20 ml) was refluxed with stirring overnight. After concentration of the solvent *in vacuo*, the residue was extracted with EtOAc, washed with saturated solution of NaHCO$_3$, brine, dried over MgSO$_4$, and concentrated under reduced pressure to yield a crude product which purified by flash chromatography using EtOAc/hexanes (1:1) then EtOAc to yield **7a or 7b**

6-chloro-2-phenethyl-2,9-dihydro-1H-pyrido[3,4-b]indol-1-one (7a).
Yield 88%; mp 265–267 °C; ν_{max} (KBr disc)/cm^{-1} 3114 (NH), 3029, 2954, 1652 (C=O), 1581, 1443, 1285, 1258, 805, 781, 745, 699; ^{1}H NMR (400 MHz, DMSO-d$_6$) δ 12.12 (s, 1H, indole NH), 8.11 (d, $J = 2.1$ Hz, 1H, Ar-H), 7.49 (d, $J = 8.7$ Hz, 1H, Ar-H), 7.38 (dd, $J = 8.8$, 2.1 Hz, 1H, Ar-H), 7.29–7.12 (m, 6H, Ar-H, CH=CHN), 6.96 (d, $J = 7.0$ Hz, 1H, CH=CHN), 4.25 (t, $J = 7.3$ Hz, 2H, NCH$_2$CH$_2$), 2.99 (t, $J = 7.3$ Hz, 2H, NCH$_2$CH$_2$); ^{13}C NMR (100 MHz, DMSO): δ 155.12 (C=O); 138.79 (C8a); 138.04 (C1'); 129.63 (C9a); 129.26 (C2', 6'); 129.07 (C3); 128.84 (C3', 5'); 126.83 (C4b); 126.72 (C4'); 124.39 (C6); 123.38 (C7); 123.23 (C5); 121.21 (C4a); 114.55 (C8); 100.16 (C4); 49.77 (NCH$_2$CH$_2$); 35.43 (NCH$_2$CH$_2$).

6-chloro-2–(4-(piperidin-1-yl)phenethyl)-2,9-dihydro-1H-pyrido[3,4-b]indol-1-one (7b).
Yield 81%; mp 293–295 °C; ν_{max} (KBr disc)/cm^{-1} 3129 (NH), 2936, 2850, 1657 (C=O), 1583, 1514, 1449, 1279, 1236, 1131, 810, 781, 754, 652; ^{1}H NMR (400 MHz, DMSO-d$_6$) δ 12.12 (s, 1H, indole NH), 8.14 (d, $J = 2.1$ Hz, 1H, Ar-H), 7.52 (d, $J = 8.7$ Hz, 1H, Ar-H), 7.41 (dd, $J = 8.8$, 2.1 Hz, 1H, Ar-H), 7.27 (d, $J = 7.0$ Hz, 1H, CH=CHN), 7.06 (d, $J = 8.5$ Hz, 2H, Ar-H), 6.99 (d, $J = 7.0$ Hz, 1H, CH=CHN), 6.83 (d, $J = 8.6$ Hz, 2H, Ar-H), 4.22 (t, $J = 7.5$ Hz, 2H, NCH$_2$CH$_2$), 3.10–3.03 (m, 4H, piperidin-H), 2.90 (t, $J = 7.5$ Hz, 2H, NCH$_2$CH$_2$), 1.65–1.46 (m, 6H, piperidin-H); ^{13}C NMR (101 MHz, DMSO-d$_6$) δ 155.08, 150.72, 138.02, 129.68, 129.65, 129.09, 128.47, 126.67, 124.36, 123.38, 123.20, 121.18, 116.35, 114.52, 100.06, 50.18, 50.03, 34.61, 25.71, 24.33; HRESI-MS m/z calcd for [M + H]$^+$ C$_{24}$H$_{25}$ClN$_3$O: 406.1681, found: 406.1676.

Biology

Appendix A has detailed information on all biological tests (Supplementary File)

Disclosure statement

No potential conflict of interest was reported by the author(s).

References

1. You W, Henneberg M. Cancer incidence increasing globally: the role of relaxed natural selection. Evol Appl. 2018;11(2): 140–152.
2. Bray F, Ferlay J, Soerjomataram I, Siegel RL, Torre LA, Jemal A. Global cancer statistics 2018: GLOBOCAN estimates of incidence and mortality worldwide for 36 cancers in 185 countries. CA Cancer J Clin. 2018;68(6):394–424.
3. Al-Sanea MM, Gotina L, Mohamed MF, Grace Thomas Parambi D, Gomaa HAM, Mathew B, Youssif BGM, Alharbi KS, Elsayed ZM, Abdelgawad MA, et al. Design, synthesis and biological evaluation of new HDAC1 and HDAC2 inhibitors endowed with ligustrazine as a novel cap moiety. Drug Des Devel Ther. 2020;14:497–508.
4. Youssif BGM, Gouda AM, Moustafa AH, Abdelhamid AA, Gomaa HAM, Kamal I, Marzouk AA. Design and synthesis of new triaryl imidazole derivatives as dual inhibitors of BRAF^{V600E}/p38α with potential antiproliferative activity. J. Mol. Struct. 2022;1253:132218.
5. Goffin JR, Zbuk K. Epidermal growth factor receptor: pathway, therapies, and pipeline. Clin Ther. 2013;35(9):1282–1303.
6. Nadeem Abbas M, Kausar S, Wang F, Zhao Y, Cui H. Advances in targeting the epidermal growth factor receptor pathway by synthetic products and its regulation by epigenetic modulators as a therapy for glioblastoma. Cells. 2019; 8(4):350–361.
7. Tebbutt N, Pedersen MW, Johns TG. Targeting the ERBB family in cancer: couples therapy. Nat Rev Cancer. 2013; 13(9):663–673.
8. Bhatia P, Sharma V, Alam O, Manaithiya A, Alam P, Alam MT, Imran M., Kahksha. Novel quinazoline-based EGFR kinase inhibitors: a review focusing on SAR and molecular docking studies (2015-2019). Eur J Med Chem. 2020;204:112640.
9. Wright NMA, Goss GD. Third-generation epidermal growth factor receptor tyrosine kinase inhibitors for the treatment of non-small cell lung cancer. Transl Lung Cancer Res. 2019; 8(Suppl 3):S247–S264.

10. Yu HA, Arcila ME, Rekhtman N, Sima CS, Zakowski MF, Pao W, Kris MG, Miller VA, Ladanyi M, Riely GJ, et al. Analysis of tumor specimens at the time of acquired resistance to EGFR-TKI therapy in 155 patients with EGFR-mutant lung cancers. Clin Cancer Res. 2013;19(8):2240–2247.

11. Walter AO, Sjin RTT, Haringsma HJ, Ohashi K, Sun J, Lee K, Dubrovskiy A, Labenski M, Zhu Z, Wang Z, et al. Discovery of a mutant-selective covalent inhibitor of EGFR that overcomes T790M-mediated resistance in NSCLC. Cancer Discov. 2013;3(12):1404–1415.

12. Patel H, Pawara R, Ansari A, Surana S. Recent updates on third generation EGFR inhibitors and emergence of fourth generation EGFR inhibitors to combat C797S resistance. Eur J Med Chem. 2017;142:32–47.

13. Shen J, Zhang T, Zhu S-J, Sun M, Tong L, Lai M, Zhang R, Xu W, Wu R, Ding J, et al. Structure-based design of 5- methyl-pyrimidopyridone derivatives as new wild-type sparing inhibitors of the epidermal growth factor receptor triple mutant (EGFR(L858R/T790M/C797S)). J Med Chem. 2019; 62(15):7302–7308.

14. Mishra RDLA. Anticancer potential of plants and natural products: a review. J. Ethnopharmacol. 2013;1:622–628.

15. Youssif BGM, Abdelrahman MH, Abdelazeem AH, Abdelgawad MA, Ibrahim HM, Salem OIA, Mohamed MFA, Treambleau L, Bukhari SNA. Design, synthesis, mechanistic and histopathological studies of small-molecules of novel indole-2-carboxamides and pyrazino[1,2-a]indol-1(2H)-ones as potential anticancer agents effecting the reactive oxygen species production. Eur J Med Chem. 2018;146:260–273.

16. Abdelrahman MH, Aboraia AS, Youssif BGM, Elsadek BEM. Design, Synthesis and Pharmacophoric Model Building of New 3-Alkoxymethyl/3-Phenyl indole-2-carboxamides with Potential Antiproliferative Activity. Chem Biol Drug Des. 2017;90(1):64–82.

17. Al-Wahaibi LH, Gouda AM, Abou-Ghadir OF, Salem OIA, Ali AT, Farghaly HS, Abdelrahman MH, Trembleau L, Abdu-Allah HHM, Youssif BGM, et al. Design and synthesis of novel 2,3-dihydropyrazino[1,2-a]indole-1,4-dione derivatives as antiproliferative EGFR and BRAF^{V600E} dual inhibitors. Bioorg Chem. 2020;104:104260.

18. Li W, Qi Y-Y, Wang Y-Y, Gan Y-Y, Shao L-H, Zhang L-Q, Tang Z-H, Zhu M, Tang S-Y, Wang Z-C, et al. Design, synthesis, and biological evaluation of sorafenib derivatives containing indole (ketone) semicarbazide analogs as antitumor agents. J Heterocyclic Chem. 2020;57(6):2548–2560.

19. Singh PK, Silakari O. Molecular dynamics guided development of indole based dual inhibitors of EGFR (T790M) and c-MET. Bioorg Chem. 2018;79:163–170.

20. Song J, Yoo J, Kwon A, Kim D, Nguyen HK, Lee B-Y, Suh W, Min KH. Structure-Activity Relationship of Indole-Tethered Pyrimidine Derivatives that Concurrently Inhibit Epidermal Growth Factor Receptor and Other Angiokinases. PLoS One. 2015;10(9):e0138823.

21. Zhang H. Three generations of epidermal growth factor receptor tyrosine kinase inhibitors developed to revolutionize the therapy of lung cancer. Drug Des Devel Ther. 2016; 10:3867–3872.

22. Mohamed FAM, Gomaa HAM, Hendawy OM, Ali AT, Farghaly HS, Gouda AM, Abdelazeem AH, Abdelrahman MH, Trembleau L, Youssif BGM, et al. Design, synthesis, and biological evaluation of novel EGFR inhibitors containing 5-chloro-3-hydroxymethyl-indole-2-carboxamide scaffold

23. with apoptotic antiproliferative activity. Bioorg Chem. 2021; 112:104960.

23. Mostafa HA, Alaa AKMH, Laurent KT. Synthesis and molecular docking of novel indole-2-carboxamide derivatives with anti-inflammatory and antinociceptive activities. J. Adv. Chem. 2014;10:3143–3159.

24. Gomaa HAM, Shaker ME, Alzarea SI, Hendawy OM, Mohamed FAM, Gouda AM, Ali AT, Morcoss MM, Abdelrahman MH, Trembleau L, et al. Optimization and SAR investigation of novel 2,3-dihydropyrazino[1,2-a]indole-1,4-dione derivatives as EGFR and BRAF^{V600E} dual inhibitors with potent antiproliferative and antioxidant activities. Bioorg Chem. 2022;120:105616.

25. Youssif BGM, Mohamed AM, Osman EEA, Abou-Ghadir OF, Elnaggar DH, Abdelrahman MH, Treamblu L, Gomaa HAM. 5-chlorobenzofuran-2-carboxamides: from allosteric CB1 modulators to potential apoptotic antitumor agents. Eur J Med Chem. 2019;177:1–11.

26. Mohassab AM, Hassan HA, Abdelhamid D, Gouda AM, Youssif BGM, Tateishi H, Fujita M, Otsuka M, Abdel-Aziz M. Design and Synthesis of Novel quinoline/chalcone/1,2,4-triazole hybrids as potent antiproliferative agent targeting EGFR and BRAF^{V600E} kinases. Bioorg Chem. 2021;106:104510.

27. Mekheimer RA, Allam SMR, Al-Sheikh MA, Moustafa MS, Al-Mousawi SM, Mostafa YA, Youssif BGM, Gomaa HAM, Hayallah AM, Abdelaziz M, et al. Discovery of new pyrimido[5,4-c]quinolines as potential antiproliferative agents with multitarget actions: Rapid synthesis, docking, and ADME studies. Bioorg Chem. 2022;121:105693.

28. Ramadan M, Abd El-Aziz M, Elshaier YAMM, Youssif BGM, Brown AB, Fathy HM, Aly AA. Design and synthesis of new pyranoquinolinone heteroannulated to triazolopyrimidine of potential apoptotic antiproliferative activity. Bioorg Chem. 2020;105:104392.

29. El-Sherief HAM, Youssif BGM, Abdelazeem AH, Abdel-Aziz M, Abdel-Rahman HM. Design, Synthesis and Antiproliferative Evaluation of Novel 1,2,4-Triazole/Schiff Base Hybrids with EGFR and B-RAF Inhibitory Activities. Anticancer Agents Med Chem. 2019;19(5):697–706.

30. Abdel-Aziz SA, Taher ES, Lan P, Asaad GF, Gomaa HAM, El-Koussi NA, Youssif BGM. Design, synthesis, and biological evaluation of new pyrimidine-5-carbonitrile derivatives bearing 1,3-thiazole moiety as novel anti-inflammatory EGFR inhibitors with cardiac safety profile. Bioorg. Chem. 2021; 111:104890.

31. Zhang B, Liu Z, Xia S, Liu Q, Gou S. Design, synthesis, and biological evaluation of sulfamoyl phenyl quinazoline derivatives as potential EGFR/CAIX dual inhibitors. Eur J Med Chem. 2021;216:113300.

32. Abou-Zied HA, Youssif BGM, Mohamed MFA, Hayallah AM, Abdel-Aziz M. EGFR inhibitors and apoptotic inducers: Design, synthesis, anticancer activity and docking studies of novel xanthine derivatives carrying chalcone moiety as hybrid molecules. Bioorg Chem. 2019;89:102997.

33. Martin SJ. Caspases: executioners of apoptosis. Pathobiol Hum Dis. 2014;145:145–152.

34. Rudel T. Caspase inhibitors in prevention of apoptosis. Herz. 1999;24(3):236–241.

35. Chemical Computing Group ULC, 1010 Sherbooke St. West, Suite #910, Montreal, QC, Canada, H3A 2R7, 2020.

36. Stamos J, Sliwkowski MX, Eigenbrot C. Structure of the epidermal growth factor receptor kinase domain alone and in

complex with a 4-anilinoquinazoline inhibitor. J Biol Chem. 2002;277(48):46265–46272.

37. Ibrahim TS, Bokhtia RM, Al-Mahmoudy AMM, Taher ES, AlAwadh MA, Elagawany M, Abdel-Aal EH, Panda S, Gouda AM, Asfour HZ, et al. Design, Synthesis and Biological Evaluation of Novel 5-((substituted quinolin-3-yl/1-naphthyl)-methylene)-3-substituted imidazolidin-2,4-dione as HIV-1 Fusion Inhibitors. Bioorg Chem. 2020;99:103782. [InsertedFromOnlin

38. Shaykoon MS, Marzouk AA, Soltan OM, Wanas AS, Radwan MM, Gouda AM, Youssif BGM, Abdel-Aziz M. Design, synthesis and antitrypanosomal activity of heteroaryl-based 1,2,4-triazole and 1,3,4-oxadiazole derivatives. Bioorg Chem. 2020;100:103933.

39. Engel J, Becker C, Lategahn J, Keul M, Ketzer J, Mühlenberg T, Kollipara L, Schultz-Fademrecht C, Zahedi RP, Bauer S, et al. Insight into the Inhibition of Drug-Resistant Mutants of the Receptor Tyrosine Kinase EGFR. Angew Chem Int Ed. (36)2016;55:10909–10912.

40. Daina A, Michielin O, Zoete V. SwissADME: a free web tool to evaluate pharmacokinetics, drug-likeness and medicinal chemistry friendliness of small molecules. Sci Rep. 2017;7: 42717.